J. Cent. South Univ. (2020) 27: 1477−1483
DOI: https://doi.org/10.1007/s11771-020-4383-1

Springer

Changes of microbial diversity during pyrite bioleaching

YIN Lu(殷璐), YANG Hong-ying(杨洪英), LI Xiang(李想), TONG Lin-lin(佟琳琳), JIN Zhe-nan(金哲男), ZHANG Qin(张勤)

School of Metallurgy, Northeastern University, Shenyang 110819, China

Abstract: Microorganisms, one of the key factors affecting the bioleaching process, change the components of extracellular polymeric substance (EPS) and community structure to survive in leaching environments. In this work, Fourier transform infrared (FTIR), X-ray powder diffraction (XRD) and 16S rDNA high-throughput sequence analyses were used to reveal the microbial changes in planktonic and sessile phases during bioleaching. The results showed the occupation of sessile cells decreased from 66.2% to (10±3)%. After bioleaching, the planktonic and sessile cells have similar EPS, but they are different from the original cells. Pyrite dissolution mainly occurs at the early and late stages with the decreasing of particle diameter, by 50% and 40%, respectively. The 16S rDNA gene based sequence analysis results in total of 1117420 Reads across the six samples, presented among 7 phyla, 9 classes, 17 orders, 23 families and 31 genera. Genera *Leptospirillum* and *Sulfobacillus* are the main bacteria at the early and middle stages, and *Leptospirillum* is the main genus at the end of bioleaching. *Aquabacterium* and *Acidovorax* are special genera in sessile cells and *Weissella* is special in planktonic ones.

Key words: pyrite dissolution; sessile cells; planktonic cells; high-throughput sequence analysis; microbial diversity; bioleaching stage

Cite this article as: YIN Lu, YANG Hong-ying, LI Xiang, TONG Lin-lin, JIN Zhe-nan, ZHANG Qin. Changes of microbial diversity during pyrite bioleaching [J]. Journal of Central South University, 2020, 27(5): 1477−1483. DOI: https://doi.org/10.1007/s11771-020-4383-1.

1 Introduction

Bioleaching can be widely applied in mining to win or concentrate precious metal, such as gold, from insoluble metal sulfides by biochemical oxidation [1]. During bioleaching process, microorganisms are characterized as physiologically and behaviorally integrated, highly structured microbial communities [2]. The cells undergo profound change significantly when they transfer from planktonic phase to part of the sessile phase.

The researches on pyrite bioleaching can be separated into two parts: mineral part and microbial part. For the mineral part, they focused on metal recovery [3], changes of mineral phases and the chemical compounds of the mineral surfaces [4]. Among the sulfides, pyrite has attracted much attention due to its stable structure and high iron and sulfur contents [5]. As a result of oxidation, jarosite and oxy-hydroxides can be detected in the samples [6]. YANG et al [7] found that silver ions could inhibit passivation layer formation on the chalcopyrite surface. YANG et al [8] also found that additional jarosite could inhibit passivation layer formation on chalcopyrite surface. For the microbial part, they focused on extracellular polymeric substance (EPS), microbial diversity and oxidation pathway. For this part, most of them

Foundation item: Project(U1608254) supported by the Special Fund for the National Natural Science Foundation of China; Projects(ZJKY2017(B)KFJJ01, ZJKY2017(B)KFJJ02) supported by the Zijin Mining Group Co., Ltd., China
Received date: 2019-06-29; **Accepted date:** 2020-04-20
Corresponding author: YANG Hong-ying, PhD, Professor; E-mail: yanghy@smm.neu.edu.cn

believed that the microorganisms oxidized pyrite via thiosulphate [9], and EPS played an important role in sulfides dissolution [10].

For the both parts, researchers share the same opinion that the microorganisms can be separated into two parts: planktonic and sessile cells. The cells attach to minerals and form biofilms which can accelerate the dissolution. LI et al [11] analyzed the constituents and chemical components changes of EPS collected from planktonic and sessile cells and the results showed that both the constituents and chemical components of EPS are different in plankton and sessile cells. It is necessary to study the bacteria behavior in pyrite bioleaching to learn the cooperation mechanism of mixed culture.

2 Experimental

2.1 Minerals and microorganisms

Pyrite used in this study was ground in a ball grinder for 10 min and more than 80% of the minerals were less than 74 μm in particle diameter. Atomic absorption spectrometry analysis showed that after nitrolysis the sample contained 45.02% Fe and 53.50% S. The main original genera in mixed culture were *Acidiplasma*, *Ferroplasma*, *Leptospirillum* and *Sulfobacillus*.

2.2 Bioleaching

The bioleaching tests were carried out in a 4.5 L bioleaching assay with 3 L mixed culture with pH=1.50±0.05. The co-culture containing $(1.8\pm0.3)\times10^8$ cells/mL was kept in 9K medium with initial pH of 1.8 at 45 °C. The medium consisted of 3 g/L $(NH_4)_2SO_4$, 0.5 g/L K_2HPO_4, 0.5 g/L $MgSO_4\cdot7H_2O$, 0.01 g/L $Ca(NO_3)_2$, 0.1 g/L KCl and 44.3 g/L $FeSO_4$ and 10% inoculation of cell suspensions [12]. Solutions were collected at the beginning, middle and end of bioleaching, for FTIR microspectroscopy, X-ray powder diffraction (XRD), 16S high-throughput sequence and chemical concentration measurements.

For the purpose of analysis, the solutions and mineral powder were examined separately. Before analyzing, powder obtained from the solution was washed with deionized water and 1 mol/L HCl and then dried at 80 °C for 8 h before characterizing by XRD (Model Ultima IV) and laser particle size analyzer (Mastersizer 3000). Besides, at the end of each special leaching experiment, the microorganisms were filtered from leaching solution through filters and rinsed with PBS solution, and then dried to analysis.

2.3 ATR FTIR spectroscopy

The chemical compositions were examined by attenuated total reflection Fourier transform infrared (ATR FTIR) spectroscopy using a Nicolet iS10 spectrometer (Thermo Fisher Scientific Crop., USA) with an average of 43 scans in the range of 400−4000 cm^{-1}.

2.4 16S high-throughput sequence

The samples for sessile and planktonic cells were filtered through millipore filter units (0.22 μm pore size) and kept at −80 °C for 16S high-throughput sequence analysis. The microorganisms were analyzed by GENEWIZ Inc., Suzhou, China. V3 and V4 regions of prokaryotic 16S rDNA were selected for PCR-amplified (the primers were CCTACGGRRBGCAS-CAGKVRVGAAT and GGACTACNVGGGTWTCTAATCC) and paired-end sequenced on an Illumina MiSeq platform after quality inspection by Qubit2.0 Fluorometer (Invitrogen, Carlsbad, CA).

3 Results

3.1 Bioleaching characterization

Redox potential, pH values and the distribution of sessile and planktonic cell per milliliter during bio-oxidization by mixed culture of acidophil are presented in Figure 1. The original pH value and redox potential were controlled as 1.70±0.05 and (455±5) mV, respectively.

Figure 1(a) indicates that the oxidation−redox potential increased from (455±5) mV to (652±10) mV and pH value decreased from 1.70±0.05 to 1.13±0.02. In Figure 1(b), at first the distribution content of sessile cells was 66.2% which was twice that of planktonic cells but 2 d later free cells occupied more than sessile ones. At the end of bioleaching, the planktonic cells occupied (90±3)%, which may result from the dissolution and weight decrement of pyrite. In bioleaching, sessile cells are much easier to get energy and share more responsibility for mineral dissolution. The chemical compounds of minerals are different before and after bioleaching, which will influence the

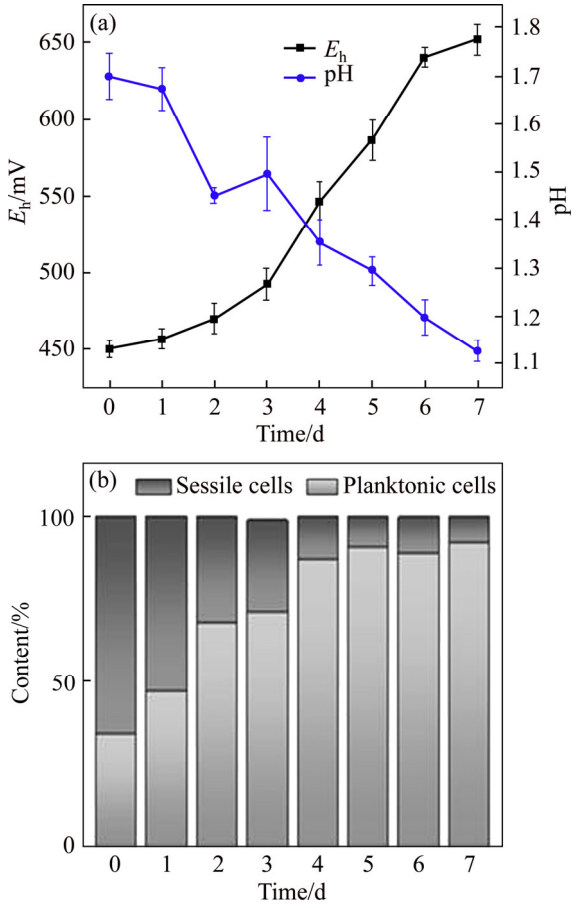

Figure 1 E_h–pH (a) and cell distribution (b) during pyrite bioleaching

composition and contents of EPS compounds. It is necessary to analyze the EPS compounds before and after bioleaching.

3.2 Biofilm composition

The FTIR spectra of cells before and after bioleaching are shown in Figure 2. After bioleaching, the spectra showed similar transmittance, which indicates the similar EPS composition. FLEMMING [13] pointed out that polysaccharides, proteins, amphiphilic molecules and DNA are involved in the first step of colonization by planktonic cells to surfaces, and the function of EPS components is to promote adhesion. The assignments of peaks indicate that cell surface consists of extracellular polysaccharides, proteins, and nucleic acids [14, 15]. Suitable contents of soluble ferrous salts render the bacteria to attach to the solid energy source, such as sulfides for growth, which results in the synthesis of more proteinaceous substances for the purpose of facilitating adhesion [16−18]. Thus, different

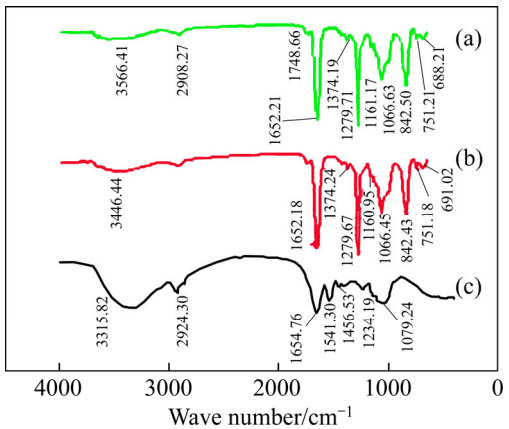

Figure 2 FTIR spectra of cells before bioleaching (a) and sessile (b) and planktonic (c)

contents of EPS components should be responsible for different adhesion forces.

As shown in Figure 2, the most remarkable difference in the peak assignments is that after bioleaching the phosphodiesters in phospholipids (1279 and 1066 cm^{-1}) are proved to be apparent on the surface of microorganisms, while polysaccharides (1160.95 cm^{-1}) are were not as significant as that of phospholipids. GEHRKE et al [17] found that the difference of ratio of total polysaccharides to proteins strongly affects the attachment of microorganisms onto solid surface. DIAO et al [19] also proposed that distinct retraction patterns captured the sequential unfolding or detachment of multiple biopolymer chains or cell surface appendages (e.g. pili and flagella). This could explain why microorganisms adapt with pyrite (FeS_2) are more hydrophobic than that with ferrous ion [20]. Besides after bioleaching, the stretching vibration band of —NH_2 (3406.24 cm^{-1}) and antisymmetric stretching vibration band of —CH_3 and —CH_2 (2924.30 cm^{-1}) became weaker.

It is of significance that the EPS compounds of both sessile cells and planktonic cells are quite different from those of the original ones. Combined with the curves of redox potential and distribution of planktonic cells, it is obvious that the bioleaching process can be separated into three phases, namely, early stage (0−3 d), middle stage (3−6 d) and late stage (6−7 d). It is necessary to analyze the chemical constitution of pyrite during bioleaching.

3.3 Mineral characterization

In bioleaching, minerals were oxidized by

microorganisms and dissolved into solution. In this work, 80% of pyrite dissolved in solution after bioleaching. The mineral phases detected by XRD and particle size analyses during bioleaching are shown in Figure 3.

As shown in Figure 3(a), the main phase is pyrite, but with the dissolution of pyrite, quartz can be detected. From Figure 3(b) and Table 1, it is significant that the content of iron(II) decreased from 45.0% to 39.8% and that of sulfur increased from 53.0% to 56.1%, indicating that the content of

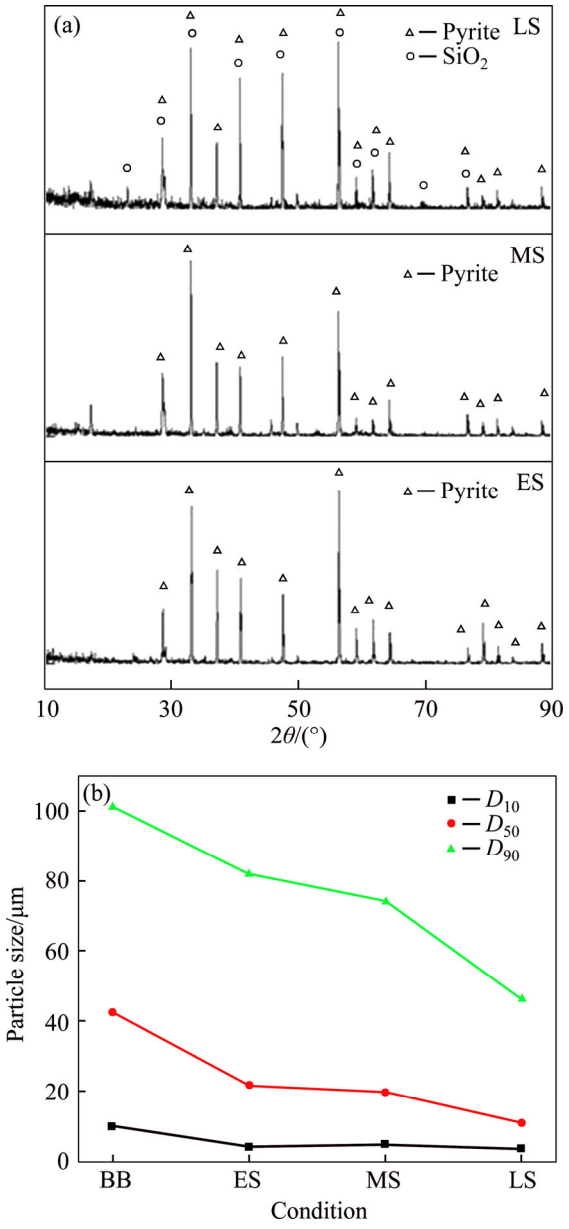

Figure 3 X-ray powder diffraction (a) and D_{10}, D_{50} and D_{90} (b) in the early, middle and late stages during pyrite bioleaching (BB: mineral before bioleaching; ES: mineral in early stage; MS: mineral in middle stage; LS: mineral in late stage)

Table 1 Contents of elemental Fe and S in pyrite during bioleaching

Condition	w(Fe)/%	w(S)/%	w(S)/w(Fe)	x(S)/x(Fe)
Original pyrite	45.00	53.00	1.18	2.07
Early stage	39.76	53.30	1.34	2.35
Middle stage	41.96	49.60	1.18	2.07
Late stage	39.83	56.10	1.41	2.46

nutrient substance changed little. From Figure 3(b), the diameter of pyrite particles decreased a little because of dissolution. D_{90}, D_{50} and D_{10} of pyrite decreased by 54.26%, 74.06% and 61.29%, respectively. Half of the pyrite particle decreased by 50% approximately during early stage because the mechanical activation promoted chemical reactions. From the early stage to the middle stage, the pyrite particle decreased by almost 10%, but both D_{50} and D_{90} decreased by (40±3)% from the middle to late stage. It means that the pyrite bio-dissolution resulted from late stages.

Pyrite dissolution is the result of biochemical reactions, and the microorganisms get energy from the oxidation of iron(II) and reduced sulfides. The mass fraction of Fe and S changed significantly, and the changing process of mineral composition can be written as $FeS_{2.07}\rightarrow FeS_{2.35}\rightarrow FeS_{2.07}\rightarrow FeS_{2.46}$. From the changing process, it is easy to find that the dissolution extents of Fe and S were different during each bioleaching stage. This may be the result of difference in community structure of microorganisms.

3.4 Microbial community structure

For the analysis of the microbial community structure, samples were analyzed and the indices of Reads, OTUs, Chao1 and the Shannon indices were calculated (Table 2). The number of OTUs (operational taxonomic unit) for each sample was 43727 based on Reads. The microbial richness of the sessile cells was greater than that of the planktonic cells, as validated by the Chao1 and Shannon indices.

The 16S rDNA gene based sequence analysis resulted in total of 1117420 Reads across the six samples, presented among 7 phyla, 9 classes, 17 orders, 23 families and 31 genera. The heat map used in this work to reflect the changes biodiversity

Table 2 Reads, OTUs, Chao1 and Shannon indices of cells collected at early stage, middle stage and late stage (SC=sessile cells and PC=planktonic cells)

Sample	Reads	OTUs	Chao1	Shannon
PC at early stage	249020	43727	25	2.299
SC at early stage	122512	43727	37	3.1
PC at middle stage	221570	43727	26	1.019
SC at middle stage	148296	43727	39.333	1.455
PC at late stage	252314	43727	26.75	0.68
SC at late stage	123708	43727	33.6	0.088 9

is shown in Figure 4. Phyla *Nitrospirae* and *Firmicutes* are the dominant, followed by *Proteobacteria*, *Bacteroidetes* and *Cyanobacteria*. 262362 OTUs were detected and 135485 OTUs and 86032 OTUs belonged to *Leptospirillum* and *Sulfobacillus*, respectively.

For genus *Leptospirillum*, the amount of OTUs was 11722 at the beginning of bioleaching, and among them 86% belonged to sessile cells. At the middle stage, this amount increased to 40318, and 59% belonged to sessile cells. At the end of bioleaching, this number increased to 83037, and 52% was for sessile. For genus *Sulfobacillus*, the OTU amount increased from 39606 to 43779 and then decreased to 2388. The occupation of sessile cells increased from 34% to 38% and finally decreased to 0.4%. It is significant that for both planktonic and sessile cells, *Leptospirillum* accumulated but *Sulfobacillus* decreased throughout the bioleaching. During bioleaching, the biodiversity showed little change, and the only change was the ratio of these genera.

To reflect the difference of microbial diversity between planktonic and sessile cells, metastats variation analysis was used in this work. The result of the analysis for the useful microorganisms is shown in Table 3. The most remarkable difference is the genus *Aquabacterium* and *Weissella*. The abundant genera *Leptospirillum* and *Sulfobacillus* showed high similarity with the p values of 0.870357 and 0.834071, respectively. The archaea *Acidiplasma* showed the highest similarity in this work. *Leptospirillum*, *Sulfobacillus* and *Acidiplasma* grew in polluted sites with high

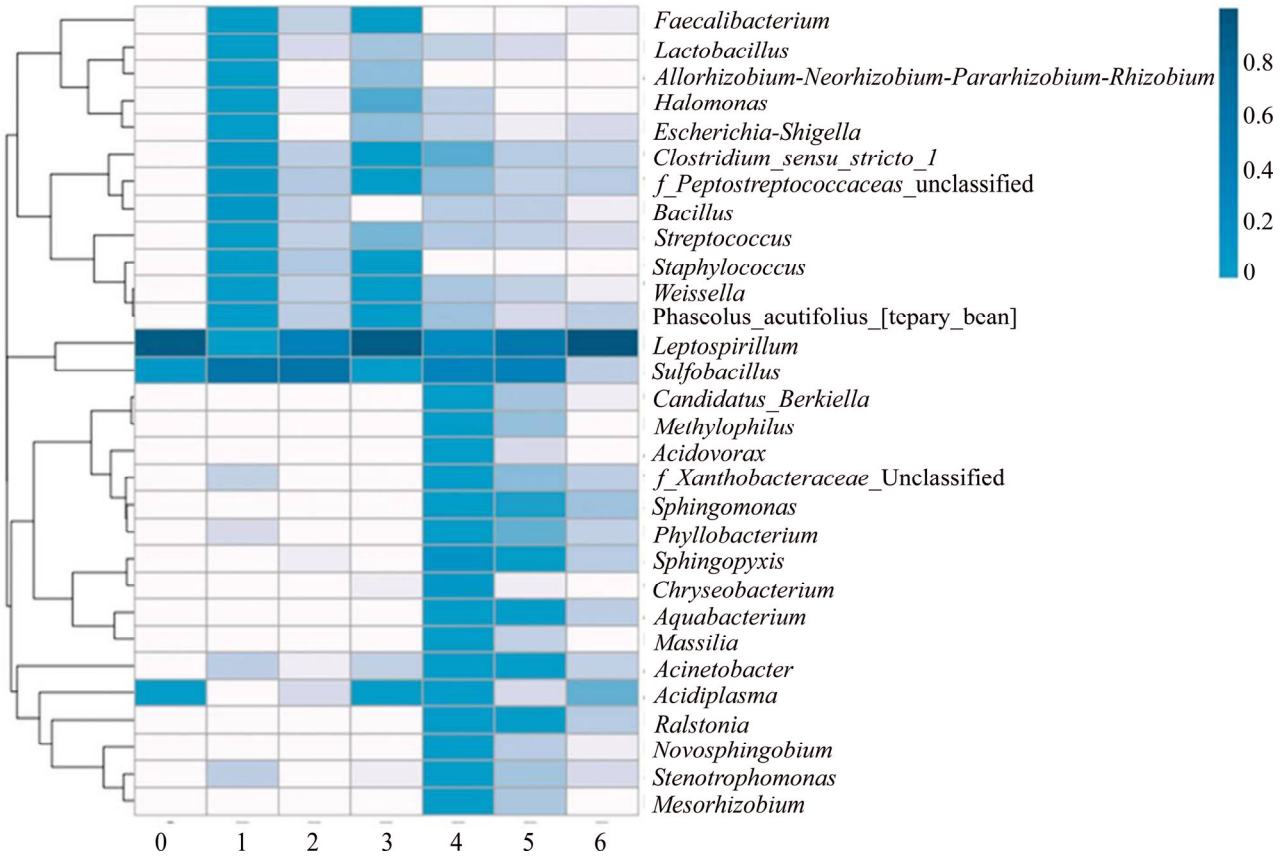

Figure 4 Heat map of cells collected at early stage, middle stage and late stage in gene level: 0−The original cells; 1−Sessile cells at early stage; 2−Sessile cells at middle stage; 3−Sessile cells at late stage; 4−Plank-tonic cells at early stage; 5−Planktonic cells at middle stage; 6−Planktonic cells at late stage

Table 3 Metastats variation analysis results calculated by language *R* (SC=sessile cells and PC=planktonic cells)

Taxon	SC_mean	SC_variance	PC_mean	PC_variance	*p*_value
Leptospirillum	0.592658876	0.147422321	0.440324422	0.193485813	0.870357
Sulfobacillus	0.231589846	0.041370683	0.42434972	0.102794592	0.834071
Aquabacterium	0.018735227	0.000782179	0	0	0.038929
Bacillus	0.000166683	2.3338×10^{-8}	0.020704141	0.001279782	0.467857143
Weissella	0.000166683	8.335×10^{-8}	0.01080209	0.000283385	0.181071
Acidiplasma	0.001066903	9.43613×10^{-7}	0.000566723	9.63526×10^{-7}	1
Acidovorax	0.00570057	9.57892×10^{-5}	0	0	0.499165

concentrations of toxic metal ions, such as tailings and acid mine drainage systems, and the main catalysts of bioleaching [19]. A similar high accumulation has been reported for eight transcriptional active acid mineral drainage taxa [20].

4 Conclusions

1) In pyrite bioleaching, redox potential increased from (455±5) mV to (652±10) mV, and pH value decreased from 1.70±0.05 to 1.13±0.02. The microorganisms can be separated into two parts: sessile cells and planktonic cells. At first, the sessile community occupied 66.2%, and with pyrite dissolution it decreased to (10±3)%. After bioleaching, the spectra showed similar transmittance, indicating similar EPS, but they are different from the original cells. The biomass contains more proteinaceous, phospholipids and polysaccharides after bioleaching.

2) Pyrite dissolution mainly occurs at the early and late stages with the decreasing of particle diameter of 50% and 40%, respectively. The chemical elements Fe and S share different dissolution extents as a result of microbial diversity. Genera *Leptospirillum* and *Sulfobacillus* are the main important bacteria at early and middle stages for both planktonic and sessile communities and *Leptospirillum* is the main genera at late stage. *Aquabacterium* and *Acidovorax* are special genera in sessile cells and *Weissella* is special in planktonic ones.

References

[1] BOSECKER K. Bioleaching: Metal solubilization by microorganisms [J]. Fems Microbiology Reviews, 1997, 20(3, 4): 591−604. DOI: 10.1111/j.1574-6976.1997.tb00340.x.

[2] MARTÍNEZ L C, VADYVALOO V. Mechanisms of post-transcriptional gene regulation in bacterial biofilms [J]. Frontiers in Cellular & Infection Microbiology, 2014, 4(4): 38. DOI: 10.3389/fcimb.2014.00038.

[3] LUO W J, YANG H Y, JIN Z N. Study on the gold recovery of double refractory gold ore concentrate by biological oxidation pretreatment [J]. Advanced Materials Research, 2015, 1130: 379−382. DOI: 10.4028/www.scientific.net/AMR.1130.379.

[4] CUI R C, YANG H Y, CHEN S, ZHANG S, LI K F. Valence variation of arsenic in bioleaching process of arsenic-bearing gold ore [J]. Transactions of Nonferrous Metals Society of China, 2010, 20(6): 1171−1176. DOI: 10.1016/S1003-6326(09)60274-0.

[5] NAYAK B. Mineral matter and the nature of pyrite in some high-sulfur tertiary coals of Meghalaya, northeast India [J]. Journal of the Geological Society of India, 2013, 81(2): 203−214. DOI: 10.1007/s12594-013-0023-9.

[6] BEVILLQUA D, LAHTI H, P SUEGAMA H, GARAIA J O, ASSIS V B, JAAKKO A P, OLLI H T. Effect of Na-chloride on the bioleaching of a chalcopyrite concentrate in shake flasks and stirred tank bioreactors [J]. Hydrometallurgy, 2013, 138(113): 1−13. DOI: 10.1016/j.hydromet.2013.06.008.

[7] YANG B, ZHAO C X, LUO W, LIAO R, GAN M, WANG J, LIU X, QIU G. Catalytic effect of silver on copper release from chalcopyrite mediated by *Acidithiobacillus ferrooxidans* [J]. J Hazard Mater, 2020, 392: 122290. DOI: 10.1016/j.jhazmat.2020.122290.

[8] YANG B, LIN M, FANG J, ZHANG R, LUO W, WANG X, LIAO R, WU B, WANG J, GAN M, LIU B, ZHANG Y, LIU X, QIN W, QIU G. Combined effects of jarosite and visible lighton chalcopyrite dissolution mediated by *Acidithiobacillus ferrooxidans* [J]. Sci Total Environ, 2020, 698: 134175. DOI: 10.1016/j.scitotenv.2019.134175.

[9] SCHIPPERS A, SAND W. Bacterial leaching of metal sulfides proceeds by two indirect mechanisms via thiosulfate or via polysulfides and sulfur [J]. Applied & Environmental Microbiology, 1999, 65(1): 319. DOI: 10.1128/AEM.65.1.319-321.1999.

[10] HENRICI A T, JOHNSON D E. Studies of freshwater bacteria: II. stalked bacteria, a new order of schizomycetes [J]. Journal of Bacteriology, 1935, 30(1): 61. DOI: 10.1002/path.1700410212.

[11] LI Q, SAND W. Mechanical and chemical studies on EPS from *Sulfobacillus thermosulfidooxidans*: From planktonic to biofilm cells [J]. Colloids & Surfaces B Biointerfaces, 2017, 153(Complete): 34−40. DOI: 10.1016/j.colsurfb.2017.02.009.

[12] DENG Sha, GU Guo-hua, WU Zi-teng, XU Xiong-yi. Bioleaching of arsenopyrite by mixed cultures of iron-oxidizing and sulfur-oxidizing microorganisms [J]. Chemosphere, 2017, 185: 403−411. DOI: 10.1016/j.chemosphere.2017.07.037.

[13] FLEMMING H C. The perfect slime [J]. Colloids & Surfaces B: Biointerfaces, 2011, 86(2): 251−259. DOI: 10.1016/j.colsurfb.2011.04.025.

[14] KIWI J, NADTOCHENKO V. Evidence for the mechanism of photocatalytic degradation of the bacterial wall membrane at the TiO_2 interface by ATR-FTIR and laser kinetic spectroscopy [J]. Langmuir, 2005, 21(10): 4631−4641. DOI: 10.1021/la0469831.

[15] VILINSKA A, RAO K H. Surface characterization of acidithiobacillus ferrooxidans adapted to high copper and zinc ions concentration [J]. Geomicrobiology Journal, 2011, 28(3): 221−228. DOI: 10.1080/01490451.2010.489920.

[16] XIA L, SHEN Z, VARGAS T, SUN W, RUAN R, XIE Z, QIU G. Attachment of Acidithiobacillus ferrooxidans onto different solid, substrates and fitting through Langmuir and Freundlich equations [J]. Biotechnology Letters, 2013, 35(12): 2129−2136. DOI: 10.1007/s10529-013-1316-1.

[17] GEHRKE T, TELEGDI J, THIERRY D. Importance of extracellular polymeric substances from *Thiobacillus ferrooxidans* for bioleaching [J]. Applied & Environmental Microbiology, 1998, 64(7): 2743−2747. DOI: 10.0000/PMID9647862.

[18] SHARMA P K, DAS A, RAO K H, FORSSBERG K S E. Surface characterization of *Acidithiobacillus ferrooxidans* cells grown under different conditions [J]. Hydrometallurgy, 2003, 71(1): 285−292. DOI: 10.0000/PMID9647862.

[19] DIAO Meng-xue, NGUYEN T A H, TARAN E, MAHLER S, NGUYEN A V. Differences in adhesion of *A. thiooxidans* and *A. ferrooxidans* on chalcopyrite as revealed by atomic force microscopy with bacterial probes [J]. Minerals Engineering, 2014, 61(6): 9−15. DOI: 10.1016/j.mineng.2014.03.002.

[20] DEVASIA P, NATARAJAN K A, SATHYANARAYANA D N, RAO G R. Surface chemistry of *Thiobacillus ferrooxidans* relevant to adhesion on mineral surfaces [J]. Applied and Environmental Microbiology, 1994, 59(12): 4051−4055. DOI: 10.1128/AEM.59.12.4051-4055.1993.

(Edited by YANG Hua)

中文导读

黄铁矿生物浸出过程中微生物的多样性变化

摘要：微生物是影响生物浸出过程的主要因素之一，它通过改变胞外高分子物质(EPS)的组分和群落结构来适应浸出环境。本文利用傅里叶变换红外光谱(FTIR)、X 射线粉末衍射(XRD)和 16S rDNA 高通量序列分析，揭示了生物浸出过程中游离和吸附微生物群落的变化。结果表明，吸附微生物由 66.2%下降到(10±3)%。生物浸出后的游离和吸附微生物具有相似的 EPS，但与原始状态不同。黄铁矿溶解主要发生在早期和晚期，随着粒度的减小，分别减少了 50%和 40%。基于 16S rDNA 基因的序列分析结果显示，6 个样品共有 1117420 个 Reads，分布在 7 个门、9 个纲、17 个目、23 个科、31 个属。*Leptospirillum* 和 *Sulfobacillus* 是早期和中期的主要菌种，*Leptospirillum* 是后期的主要菌属。*Aquabacterium* 和 *Acidovorax* 在吸附细胞中是特殊的属，而 *Weissella* 是游离细胞中独有的。

关键词：黄铁矿溶解；吸附细胞；游离细胞；高通量测序；微生物多样性；生物浸出阶段